Identification of a novel loss-of-function *PHEX* mutation, Ala720Ser, in a sporadic case of adult-onset hypophosphatemic osteomalacia

Katarzyna Goljanek-Whysall[a], Andreas Tridimas[b], Rachel McCormick[a], Nicki-Jayne Russell[b], Melissa Sloman[c], Alan Sorani[d], William D. Fraser[e], Fadil M. Hannan[a,b]*

[a]Department of Musculoskeletal Biology, Institute of Ageing and Chronic Disease, University of Liverpool, Liverpool, UK

[b]Department of Clinical Biochemistry and Metabolic Medicine, Royal Liverpool University Hospital, Liverpool, UK

[c]Department of Molecular Genetics, Royal Devon & Exeter NHS Hospital, Exeter, UK

[d]Department of Radiology, Royal Liverpool University Hospital, Liverpool, UK

[e]Department of Medicine, Norwich Medical School, University of East Anglia, Norwich, UK

*Corresponding author at: Department of Musculoskeletal Biology, Institute of Ageing and Chronic Disease, Apex Building, Liverpool, L7 8TX, UK.

Email address: fhannan@liverpool.ac.uk

Abstract

Adults presenting with sporadic hypophosphatemia and elevations in circulating fibroblast growth factor-23 (FGF23) concentrations are usually investigated for an acquired disorder of FGF23 excess such as tumor induced osteomalacia (TIO). However, in some cases the underlying tumor is not detected, and such patients may harbor other causes of FGF23 excess. Indeed, coding-region and 3'UTR mutations of phosphate-regulating neutral endopeptidase (*PHEX*), which encodes a cell-surface protein that regulates circulating FGF23 concentrations, can lead to alterations in phosphate homeostasis, which are not detected until adulthood. Here, we report an adult female who presented with hypophosphatemic osteomalacia and raised serum FGF23 concentrations. The patient and her parents, who were her only first-degree relatives, had no history of rickets. The patient was thus suspected of having TIO. However, no tumor had been identified following extensive localization studies. Mutational analysis of the *PHEX* coding-region and 3'UTR was undertaken, and this revealed the patient to be heterozygous for a novel germline *PHEX* mutation (c.2158G>T; p.Ala720Ser). *In vitro* studies involving the expression of WT and mutant PHEX proteins in HEK293 cells demonstrated the Ala720Ser mutation to impair trafficking of PHEX, with <20% of the mutant protein being expressed at the cell surface, compared to >80% cell surface expression for WT PHEX ($p<0.05$). Thus, our studies have identified a pathogenic *PHEX* mutation in a sporadic case of adult-onset hypophosphatemic osteomalacia, and these findings highlight a role for *PHEX* gene analysis in some cases of suspected TIO, particularly when no tumor has been identified.

Key words*:* FGF23, PHEX, X-linked, hypophosphatemia, osteomalacia, tumor

Abbreviations: ALP, alkaline phosphatase; ESR, erythrocyte sedimentation rate; EVS, Exome Variant Server; EXAC, Exome Aggregation Consortium; FDG, ^{18}fluorodeoxyglucose; FGF23, fibroblast growth factor-23; PHEX, phosphate-regulating neutral endopeptidase; PsA, psoriatic arthritis; TIO, tumor induced osteomalacia; TmP/GFR, Tubular maximum of phosphate/glomerular filtration rate; WT, wild-type; XLH, X-linked hypophosphatemia.

1. Introduction

The circulating concentration of phosphate is regulated by fibroblast growth factor-23 (FGF23), which is an osteocyte-derived hormone that influences proximal renal tubular phosphate reabsorption and the renal synthesis of 1,25-dihydroxyvitamin D (1). Primary disorders of FGF23 excess are characterized by renal tubular phosphate wasting and low serum 1,25-dihydroxyvitamin D concentrations, which lead to hypophosphatemia and impaired skeletal mineralization (1, 2). The most common inherited cause of FGF23 excess is X-linked hypophosphatemia (XLH; OMIM #307800), which has a prevalence of 1:20,000 (3), and is caused by loss-of-function mutations affecting the *PHEX* gene on chromosome Xp22.1 (4-7). *PHEX* encodes the phosphate-regulating neutral endopeptidase, which is a cell-surface protein expressed in osteocytes, osteoblasts and odontoblasts; and considered to play a role in inhibiting FGF23 synthesis (1). XLH is in general a highly penetrant X-linked dominant disorder characterized by childhood rickets, which is unresponsive to physiological doses of vitamin D, and occurs in association with growth retardation and dental abnormalities (5, 8). However, XLH can also mimic a sporadic or X-linked recessive form of rickets, which is characterized by a mild clinical phenotype, and caused by a mutation within the *PHEX* 3'-UTR region (9). In contrast to XLH, which generally manifests in the second year of life when affected individuals begin weight-bearing, patients presenting in adulthood with hypophosphatemia and elevated serum FGF-23 concentrations, in the absence of any family history of rickets, are usually investigated for an underlying acquired cause such as tumor induced osteomalacia (TIO) (10). This paraneoplastic disorder is most commonly caused by the ectopic secretion of FGF23 from benign mesenchymal tumors (11, 12). The diagnosis of TIO is often difficult as the causative mesenchymal tumors are generally small and occur in any soft tissue or bone (13). Indeed, despite extensive tumor localization studies, which may span several years and involve a range of imaging modalities such as whole body MRI, octreotide scintigraphy and ^{18}fluorodeoxyglucose PET/CT (FDG-PET/CT) (14), the underlying cause of the FGF23 excess is often not established. Here, we report a previously well patient with no known family history of rickets, who presented with hypophosphatemic osteomalacia and raised serum FGF23 concentrations in adulthood. She was

suspected as having TIO, but no tumor was detected. However, mutational analysis identified a novel germline loss-of-function *PHEX* mutation, and these findings suggest that *PHEX* mutations may account for some cases of sporadic adult-onset hypophosphatemic osteomalacia.

2. Case Report

A previously well 43-year-old woman presented with widespread psoriasis in association with a 12-month history of pain and stiffness affecting the lumbar back, hips and feet; and swelling of the metacarpophalangeal joints. She was not on any regular medications, did not take any vitamins or tonics, and had not altered her diet. She was diagnosed with a late-onset form of psoriatic arthritis (PsA) (presenting at >40 years), which accounts for ~30% of all PsA cases (15). She had a persistently raised erythrocyte sedimentation rate (ESR), ranging from 26-81 mm/hr (normal 2-19 mm/hr), which is observed in ~50% of PsA patients (16). However, her symptoms did not improve following treatment with methotrexate. Plain radiography identified Looser zones affecting the femora (Fig. 1A), and she was assumed to also have vitamin D deficient osteomalacia, and commenced on ergocalciferol 250 micrograms weekly, However, her symptoms persisted, and serum biochemistry, which was measured on a random (non-fasting) sample, following three months of treatment with ergocalciferol revealed a low phosphate of 0.43 mmol/L (normal 0.70-1.40 mmol/L), normal concentrations of albumin-adjusted calcium and creatinine, borderline elevation of alkaline phosphatase (ALP) activity, adequate 25-hydroxyvitamin D of 72.4 nmol/L (29.0 ng/mL) and raised parathyroid hormone concentration (Table 1). Tubular maximum of phosphate/glomerular filtration rate (TmP/GFR) was low at 0.40 mmol/L (normal 0.80-1.35 mmol/L), consistent with a renal tubular phosphate loss. No alterations in serum electrolytes or urate concentrations were noted (Table 1). Moreover, urinary glucose was not detected, and the urinary concentrations of amino acids and retinol binding protein were not elevated, thus indicating that the patient did not have a generalised disturbance of proximal renal tubular function. Serum 1,25-dihydroxyvitamin D was inappropriately normal, given the hypophosphatemia; at 98 pmol/L (normal 43-144 pmol/L). Serum FGF23, which was measured using the human C-terminal FGF23 ELISA (Immutopics) (17), was elevated at 779

RU/mL (normal <100 RU/mL). These findings were consistent with FGF23-mediated hypophosphatemia. She had no childhood history of rickets, and the onset of her hypophosphatemia was not known, as serum biochemical profiling had not been previously undertaken. Moreover, it was uncertain whether there was a family history of rickets as she had no children or siblings. However, her parents were not known to be of short stature or affected by any musculoskeletal disorders. She had a history of dental abscesses, which were attributed to dental trauma as a child. Her height was 150 cm (4 feet and 11 inches), which is within the normal range for women of her ethnicity (Middle Eastern origin) and corresponds to the 12th height centile. No disproportionate lower limb shortening was noted, and the upper and lower segment heights were 70cm and 80cm, respectively. No frontal bossing or other skeletal deformities were detected on examination. Mild enthesopathic changes affecting the ischial tuberosities, and an incidental finding of L5 spina bifida, were noted on a review of her plain radiographs (Fig. 1A). No abnormalities were detected on technetium 99m skeletal scintigraphy. She had no known acquired causes of FGF23 excess, such as being treated with iron infusions or having undergone a renal transplant (18, 19). Investigations for TIO, which included whole body MRI, octreotide scintigraphy and FDG-PET/CT did not detect an underlying tumor. She was commenced on oral phosphate (500 mg elemental phosphorus 2-3 times daily) and alfacalcidol 250 ng daily, which improved the hypophosphatemia and normalised the ALP activity (Fig. 1B). However, she has remained symptomatic and her serum C-terminal FGF23 concentrations have been persistently elevated (Fig. 1B). This patient has been assessed over a period of eight years with serial imaging studies for presumed TIO, and no causative tumor has been identified.

3. Methods

3.1 Genetic analysis

All genetic analyses were performed by the Department of Molecular Genetics at the Royal Devon and Exeter Hospital, UK. PCR and Sanger sequence analysis of all 22 exons of the *PHEX* gene was performed using leukocyte DNA. PCR primer sequences are available on request. *PHEX* gene dosage analysis was assessed by multiple ligation-dependent probe amplification (MLPA) using MRC Holland kit P2223-B1. Subsequent analysis of the *DMP1, ENPP1, FGF23, PHEX* and *SLC34A3* genes was undertaken by targeted next generation sequencing (Agilent custom capture v6/Illumina NextSeq500). All the coding regions and exon/intron boundaries (50 bp upstream to 10 bp downstream of each exon) were analysed for these five genes and also included the 3'UTR region of the *PHEX* gene for the detection of the reported c.*231A>G mutation (9). Publicly accessible databases including the Exome Variant Server (EVS) (http://evs.gs.washington.edu/EVS/) and the Exome Aggregation Consortium (EXAC) (http://exac.broadinstitute.org/), PHEX mutation database 'PHEXdb' (http://www.phexdb.mcgill.ca/) and HGMD Pro >(https://portal.biobase-international.com/hgmd/pro/start.php) were examined for the presence of any detected sequence variants. PHEX ortholog protein sequences were aligned using ClustalOmega (http://www.ebi.ac.uk/Tools/msa/clustalo/) (20).

3.2 Cellular analysis of PHEX protein expression

HEK293 cells were cultured in DMEM (Sigma) supplemented with 10% FBS (Invitrogen). Cells were split into 12-well plates, and transfected using Lipofectamine 2000 (Invitrogen) and vectors encoding either the full-length wild-type (WT) human PHEX (Source Bioscience; clone accession: KJ891794) or mutant PHEX (GeneArt, Invitrogen; mutation: c.2158G>T) or an empty pCS3 vector, as described (21, 22). Cells were lysed for western blotting or fixed for immunostaining 48h following transfections. HEK293 cells were lysed using RIPA buffer and denatured in Laemmli sample buffer (21). Protein separation and western blot were performed, as described (22). An anti-PHEX rabbit polyclonal antibody (Abcam, ab96072) was used at 1:500 dilution. Secondary HRP-conjugated

antibody (anti-rabbit; Cell Signalling) was used at 1:2000 dilution. Immune complexes were visualised by chemiluminescence using ECL kit (Thermo Fisher Scientific). Ponceau S staining (*Po-S, Sigma Co,*) was used to visualise the loaded protein. HEK293 cells were fixed in 4% paraformaldehyde in PBS, and immunostaining performed, as described (22). To assess for PHEX and endoplasmic reticulum (ER) co-immunostaining, cells were permeabilised with 0.5% Triton X-100. Immunostaining was performed using anti-PHEX (1:500; Abcam; ab96072), anti-Na-K-ATPase (1:100; 610992, BD Bioscience) or anti-calnexin (1:100; 610523, BD Bioscience) antibodies; and using secondary anti-mouse AlexaFluor-488 and anti-rabbit AlexaFluor-594 antibodies (Invitrogen). Cells were visualised using a Zeiss fluorescent microscope. Colocalisation quantification was performed using BioimageX (23). The percentage of PHEX immunostaining at the plasma membrane or ER was quantified using a minimum of six slides from at least four separate experiments, and compared between WT and mutant-expressing cells using the Student's t-test.

4. Results

DNA sequence analysis of the *PHEX* coding regions and adjacent splice sites identified a novel heterozygous G-to-T transversion at nucleotide c.2158 in exon 22 in the patient (Fig. 1C). This G-to-T transversion (GCA to TCA) resulted in a missense substitution, p.Ala720Ser, of the PHEX protein (Fig. 1D). The absence of this DNA sequence abnormality in >6500 exomes from the EVS cohort and >60,700 exomes from the ExAC cohort, together with evolutionary conservation of the Ala720 residue in vertebrate PHEX orthologs (Figure 1E), indicated that the Ala720Ser abnormality likely represented a pathogenic *PHEX* mutation rather than a benign polymorphic variant. No alterations in *PHEX* gene dosage or in the *PHEX* 3'UTR were identified. Moreover, analysis of the *DMP1*, *ENPP*, *FGF23* and *SLC34A3* genes, which are involved in phosphate homeostasis and have been associated with FGF23-mediated hypophosphatemia (1, 18), did not reveal any abnormalities.

PHEX proteins that harbor missense mutations have previously been shown to be sequestered intracellularly (3), and we therefore investigated whether the Ala720Ser mutation may impair the expression and cellular processing of PHEX by *in vitro* transient transfection of WT (Ala720) or

mutant (Ser720) *PHEX* full-length cDNA constructs in HEK293 cells. Western blot analysis of whole cell lysates obtained from transfected HEK293 cells demonstrated similar levels of expression of WT and mutant PHEX proteins, whereas, cells transfected with an empty vector (control) were shown to not express PHEX (Fig. 2A). Immunofluorescence analysis of permeabilised and non-permeabilised cells was undertaken to determine the cellular localization of WT and mutant PHEX proteins (Fig. 2B-C). A localisation analysis of non-permeabilised cells revealed that ~80% of the total cellular amount of WT PHEX was localised at the plasma membrane (Fig. 2B and 2D). Whereas, in permeabilised cells, less than 20% of WT PHEX was localised in the ER (Figure 2C-D). In contrast, only ~20% of the mutant Ser720 PHEX protein was localised at the plasma membrane in non-permeabilised cells (Fig. 2B and 2D), whereas greater than 60% of mutant PHEX was associated with the ER (Fig. 2C-D). These findings indicate impaired trafficking and ER retention of the mutant Ser720 PHEX protein.

5. Discussion

Our studies have identified a pathogenic *PHEX* mutation in a patient with elevated circulating FGF23 concentrations and hypophosphatemic osteomalacia that first manifested in adulthood. Although, *PHEX* mutations are occasionally detected in osteomalacic adults (24), and even in asymptomatic adults (25), such cases usually arise within a kindred known to be affected with XLH. In contrast, the patient reported here did not have a known family history of rickets or osteomalacia, which indicates that her adult-onset XLH had likely occurred sporadically. It is of note that this patient was also diagnosed with PsA, which is an inflammatory musculoskeletal disease characterised by features such as arthritis, dactylitis, psoriatic skin disease and nail dystrophy (26). Moreover, PsA has been associated with elevated serum FGF23 concentrations (27), and this may potentially have contributed to the FGF23 excess in this patient. Furthermore, she was found to have enthesopathic changes on plain radiography. Such findings have been reported in >65% of XLH patients (28) and in 30-50% of PsA patients (26), and thus the cause of the enthesopathy in this patient who is affected with both of these conditions, remains to be elucidated. In addition, she had a history of dental abscesses that

began in childhood and were attributed to prior trauma, but which may potentially have represented an early manifestation of XLH. Indeed, dental abscesses are a common feature of XLH in children and have been reported to affect the primary dentition of 25% of XLH patients (29).

The missense Ala720Ser mutation identified in this case involved the substitution of a WT non-polar alanine residue with a mutant polar serine residue, and this was predicted to result in misfolding and retention of the mutant PHEX protein within the ER (3). Indeed, >50% of XLH-causing missense PHEX mutations, which includes another mutation affecting codon 720 of the *PHEX* gene (Ala720Thr), have previously been shown to impair trafficking of the mutant PHEX protein to the plasma membrane (3). Our *in vitro* studies revealed the Ala720Ser mutation to partially abrogate cell surface expression of the PHEX protein, and these milder pathogenic effects may explain why the patient became symptomatic only in adulthood. Another contributing factor to the milder clinical phenotype may have been cellular mosaicism arising from skewed X-inactivation of the mutant *PHEX* gene (30). Although it should be noted that such skewing has not been reported in peripheral blood cells obtained from females with XLH (31), and it remains to be elucidated whether preferential inactivation of the mutant *PHEX* gene may occur in FGF23-secreting cells such as osteocytes. Some females with XLH have been reported to have an absence of skeletal disease, and the only manifestation may be asymptomatic hypophosphatemia (25). Similarly, a recent study of XLH caused by a *PHEX* 3'-UTR mutation included an assessment of the affected mothers, and their only consistent phenotype was a mild reduction in TmP/GFR, which was not associated with substantial hypophosphatemia or skeletal abnormalities (9). The findings of these previous studies and the present report highlight that *PHEX* mutations in females may not present until adulthood or could potentially go unnoticed throughout adult life (9, 25).

The present case illustrates the challenge of investigating hypophosphatemic patients with demonstrable FGF23 excess in the absence of a known family history of rickets or osteomalacia. Such patients are usually suspected of harboring an acquired disorder such as TIO (18), and may undergo radiological investigations over several years to detect the underlying tumor (14, 32). However, despite these imaging studies, the causative tumor has been reported to not be identified in 25-60% of patients with FGF23-mediated adult-onset hypophosphatemic osteomalacia (12, 14, 33), thus

indicating that some patients may harbor an alternate etiology for their mineral disorder. Our findings highlight that a monogenic cause of FGF23 excess should be considered in such cases, even in the absence of a relevant family history, and that *PHEX* gene analysis may have utility in the investigation of patients with suspected TIO, particularly when the underlying tumor has not been identified. Appropriate diagnosis in such cases will prevent unnecessary radiological investigations, although treatment with phosphate and active vitamin D may not fully alleviate symptoms. Whether anti-FGF23 antibody treatment (34) would be beneficial in such patients remains to be investigated.

Author's role:

Study design: FMH and WDF. Study conduct: FMH. Data collection: KG-W, AT, RM, N-JR, MS, AS. Data analysis and interpretation: KG-W, AT, RM, N-JR, MS, AS. Drafting manuscript: KG-W, AT, WDF, FMH: Approving final version of manuscript: all authors. FMH takes responsibility for the integrity of the data analysis.

Disclosure statement:

FMH has received honoraria from Shire Pharmaceuticals. WDF has received educational awards from Alexion and Shire; and speaker fees from Alexion, Shire, Lilly, Roche, Seimens and Abbott; and been on Advisory Boards for Alexion, Shire, Internis and Stirling Anglian Pharmaceuticals.

Acknowledgements:

This research did not receive any specific grant from funding agencies in the public, commercial, or not-for-profit sectors.

References

1. Quarles LD. Endocrine functions of bone in mineral metabolism regulation. *J Clin Invest.* 2008;118(12):3820-8.
2. Carpenter TO. In: De Groot LJ, Beck-Peccoz P, Chrousos G, Dungan K, Grossman A, Hershman JM, Koch C, McLachlan R, New M, Rebar R, et al. eds. *Endotext*. South Dartmouth (MA); 2000.
3. Sabbagh Y, Boileau G, Campos M, Carmona AK, and Tenenhouse HS. Structure and function of disease-causing missense mutations in the PHEX gene. *J Clin Endocrinol Metab.* 2003;88(5):2213-22.
4. A gene (PEX) with homologies to endopeptidases is mutated in patients with X-linked hypophosphatemic rickets. The HYP Consortium. *Nat Genet.* 1995;11(2):130-6.
5. Dixon PH, Christie PT, Wooding C, Trump D, Grieff M, Holm I, Gertner JM, Schmidtke J, Shah B, Shaw N, et al. Mutational analysis of PHEX gene in X-linked hypophosphatemia. *J Clin Endocrinol Metab.* 1998;83(10):3615-23.
6. Gaucher C, Walrant-Debray O, Nguyen TM, Esterle L, Garabedian M, and Jehan F. PHEX analysis in 118 pedigrees reveals new genetic clues in hypophosphatemic rickets. *Hum Genet.* 2009;125(4):401-11.
7. Holm IA, Nelson AE, Robinson BG, Mason RS, Marsh DJ, Cowell CT, and Carpenter TO. Mutational analysis and genotype-phenotype correlation of the PHEX gene in X-linked hypophosphatemic rickets. *J Clin Endocrinol Metab.* 2001;86(8):3889-99.
8. Carpenter TO, Imel EA, Holm IA, Jan de Beur SM, and Insogna KL. A clinician's guide to X-linked hypophosphatemia. *J Bone Miner Res.* 2011;26(7):1381-8.
9. Mumm S, Huskey M, Cajic A, Wollberg V, Zhang F, Madson KL, Wenkert D, McAlister WH, Gottesman GS, and Whyte MP. PHEX 3'-UTR c.*231A>G near the polyadenylation signal is a relatively common, mild, American mutation that masquerades as sporadic or X-linked recessive hypophosphatemic rickets. *J Bone Miner Res.* 2015;30(1):137-43.
10. Chong WH, Molinolo AA, Chen CC, and Collins MT. Tumor-induced osteomalacia. *Endocr Relat Cancer.* 2011;18(3):R53-77.
11. Bahrami A, Weiss SW, Montgomery E, Horvai AE, Jin L, Inwards CY, and Folpe AL. RT-PCR analysis for FGF23 using paraffin sections in the diagnosis of phosphaturic mesenchymal tumors with and without known tumor induced osteomalacia. *Am J Surg Pathol.* 2009;33(9):1348-54.
12. Jiang Y, Xia WB, Xing XP, Silva BC, Li M, Wang O, Zhang HB, Li F, Jing HL, Zhong DR, et al. Tumor-induced osteomalacia: an important cause of adult-onset hypophosphatemic osteomalacia in China: Report of 39 cases and review of the literature. *J Bone Miner Res.* 2012;27(9):1967-75.
13. Hannan FM, Athanasou NA, Teh J, Gibbons CL, Shine B, and Thakker RV. Oncogenic hypophosphataemic osteomalacia: biomarker roles of fibroblast growth factor 23, 1,25-dihydroxyvitamin D3 and lymphatic vessel endothelial hyaluronan receptor 1. *Eur J Endocrinol.* 2008;158(2):265-71.
14. Chong WH, Andreopoulou P, Chen CC, Reynolds J, Guthrie L, Kelly M, Gafni RI, Bhattacharyya N, Boyce AM, El-Maouche D, et al. Tumor localization and biochemical response to cure in tumor-induced osteomalacia. *J Bone Miner Res.* 2013;28(6):1386-98.
15. Queiro R, Tejon P, Alonso S, and Coto P. Age at disease onset: a key factor for understanding psoriatic disease. *Rheumatology (Oxford).* 2014;53(7):1178-85.
16. Punzi L, Podswiadek M, Oliviero F, Lonigro A, Modesti V, Ramonda R, and Todesco S. Laboratory findings in psoriatic arthritis. *Reumatismo.* 2007;59 Suppl 1:52-5.
17. Durham BH, Joseph F, Bailey LM, and Fraser WD. The association of circulating ferritin with serum concentrations of fibroblast growth factor-23 measured by three commercial assays. *Ann Clin Biochem.* 2007;44(Pt 5):463-6.
18. Imel EA, and Econs MJ. Approach to the hypophosphatemic patient. *J Clin Endocrinol Metab.* 2012;97(3):696-706.
19. Schouten BJ, Hunt PJ, Livesey JH, Frampton CM, and Soule SG. FGF23 elevation and hypophosphatemia after intravenous iron polymaltose: a prospective study. *J Clin Endocrinol Metab.* 2009;94(7):2332-7.

20. Sievers F, Wilm A, Dineen D, Gibson TJ, Karplus K, Li W, Lopez R, McWilliam H, Remmert M, Soding J, et al. Fast, scalable generation of high-quality protein multiple sequence alignments using Clustal Omega. *Mol Syst Biol.* 2011;7(539.
21. Goljanek-Whysall K, Pais H, Rathjen T, Sweetman D, Dalmay T, and Munsterberg A. Regulation of multiple target genes by miR-1 and miR-206 is pivotal for C2C12 myoblast differentiation. *J Cell Sci.* 2012;125(Pt 15):3590-600.
22. Soriano-Arroquia A, McCormick R, Molloy AP, McArdle A, and Goljanek-Whysall K. Age-related changes in miR-143-3p:Igfbp5 interactions affect muscle regeneration. *Aging Cell.* 2016;15(2):361-9.
23. Kankaanpaa P, Paavolainen L, Tiitta S, Karjalainen M, Paivarinne J, Nieminen J, Marjomaki V, Heino J, and White DJ. BioImageXD: an open, general-purpose and high-throughput image-processing platform. *Nat Methods.* 2012;9(7):683-9.
24. Econs MJ, Friedman NE, Rowe PS, Speer MC, Francis F, Strom TM, Oudet C, Smith JA, Ninomiya JT, Lee BE, et al. A PHEX gene mutation is responsible for adult-onset vitamin D-resistant hypophosphatemic osteomalacia: evidence that the disorder is not a distinct entity from X-linked hypophosphatemic rickets. *J Clin Endocrinol Metab.* 1998;83(10):3459-62.
25. Makras P, Hamdy NA, Kant SG, and Papapoulos SE. Normal growth and muscle dysfunction in X-linked hypophosphatemic rickets associated with a novel mutation in the PHEX gene. *J Clin Endocrinol Metab.* 2008;93(4):1386-9.
26. Ritchlin CT, Colbert RA, and Gladman DD. Psoriatic Arthritis. *N Engl J Med.* 2017;376(10):957-70.
27. Okan G, Baki AM, Yorulmaz E, Dogru-Abbasoglu S, and Vural P. Fibroblast Growth Factor 23 and Placental Growth Factor in Patients with Psoriasis and their Relation to Disease Severity. *Ann Clin Lab Sci.* 2016;46(2):174-9.
28. Hardy DC, Murphy WA, Siegel BA, Reid IR, and Whyte MP. X-linked hypophosphatemia in adults: prevalence of skeletal radiographic and scintigraphic features. *Radiology.* 1989;171(2):403-14.
29. McWhorter AG, and Seale NS. Prevalence of dental abscess in a population of children with vitamin D-resistant rickets. *Pediatr Dent.* 1991;13(2):91-6.
30. Migeon BR. X inactivation, female mosaicism, and sex differences in renal diseases. *J Am Soc Nephrol.* 2008;19(11):2052-9.
31. Orstavik KH, Orstavik RE, Halse J, and Knudtzon J. X chromosome inactivation pattern in female carriers of X linked hypophosphataemic rickets. *J Med Genet.* 1996;33(8):700-3.
32. Jagtap VS, Sarathi V, Lila AR, Malhotra G, Sankhe SS, Bandgar T, Menon P, and Shah NS. Tumor-induced osteomalacia: a single center experience. *Endocr Pract.* 2011;17(2):177-84.
33. Yu WJ, He JW, Fu WZ, Wang C, and Zhang ZL. Reports of 17 Chinese patients with tumor-induced osteomalacia. *J Bone Miner Metab.* 2017; 35(3):298-307.
34. Imel EA, Zhang X, Ruppe MD, Weber TJ, Klausner MA, Ito T, Vergeire M, Humphrey JS, Glorieux FH, Portale AA, et al. Prolonged Correction of Serum Phosphorus in Adults With X-Linked Hypophosphatemia Using Monthly Doses of KRN23. *J Clin Endocrinol Metab.* 2015;100(7):2565-73.

Figure legends

Figure 1. Clinical findings and *PHEX* mutational analysis. (A) Pelvic and proximal femoral radiographs showing bilateral cortical lucencies of the proximal medial femoral diaphysis with associated focal cortical thickening (yellow arrows), representing an insufficiency-type fracture or "Looser zone". Mild enthesopathic changes affecting the ischial tuberosities (red arrowheads) and an incidental finding of L5 spina bifida (black arrow) are also noted. (B) Graphs showing serum concentrations of phosphate (Pi), alkaline phosphatase (ALP) and fibroblast growth factor-23 (FGF23) over an 8-year period. Boxes above graphs indicate periods of treatment with ergocalciferol (D2), and with oral phosphate and alfacalcidol. (C) DNA sequence analysis showing a heterozygous G-to-T transversion at nucleotide c.2158 (red arrow) of the *PHEX* gene. (D) This sequence abnormality was predicted to lead to a missense amino acid substitution of Ala to Ser at codon 720. (E) Multiple protein sequence alignment of PHEX orthologs. The WT Ala720 (A) residues are shown in black, and the mutant Ser720 (S) residue is shown in red. Conserved residues are shaded grey.

Figure 2. Cellular localization of WT and mutant PHEX. (A) Western blot showing elevated levels of PHEX protein following transfection of HEK293 cells with a vector encoding WT or mutant PHEX as compared to cells transfected with an empty vector. (B) Immunofluorescence of non-permeabilised HEK293 cells showing the co-localisation of PHEX (red) with Na-K-ATPase, which is a plasma membrane-associated protein (green). (C) Immunofluorescence of permeabilised HEK293 cells showing the co-localisation of PHEX (red) with calnexin, which is an ER-associated protein (green). (D) Quantification of co-localisation of WT or mutant PHEX protein with plasma membrane or ER-associated proteins in HEK293 cells. *$p<0.05$; bars show standard deviation.

Table 1. Serum biochemical parameters at presentation.

Parameter	Value	Reference range
Sodium (mmol/L)	136	135-145
Potassium (mmol/L)	3.7	3.5-5.0
Creatinine (μmol/L)	57	54-145
Albumin-adjusted calcium (mmol/L)	2.41	2.20-2.60
Phosphate (mmol/L)	0.43	0.70-1.40
Alkaline phosphatase (U/L)	136	30-130
Urate (μmol/L)	237	140-360
Parathyroid hormone (pmol/L)	11	1.1-6.9
25-hydroxyvitamin D (nmol/L)	72.4	Adequate >50
1,25-dihydroxyvitamin D (pmol/L)	98	43-144
FGF23 (RU/mL)	779	<100

Figure 1

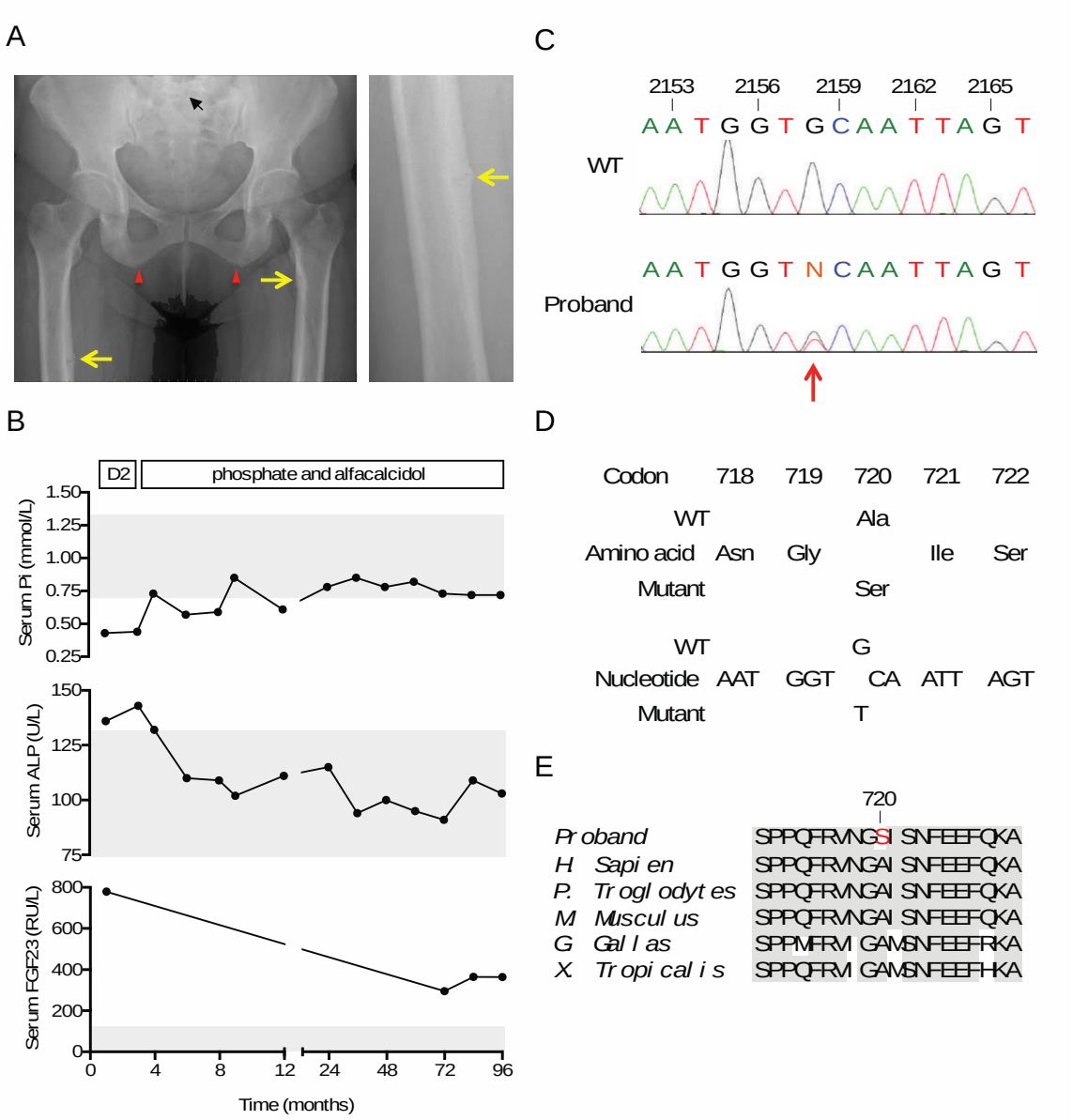
A
C
2153
2156
2159
2162
2165
A A T G G T G C A A T T A G T
WT
A A T G G T N C A A T T A G T
Proband
B
D2
phosphate and alfacalcidol
Serum Pi (mmol/L)
1.50
1.25
1.00
0.75
0.50
0.25
Serum ALP (U/L)
150
125
100
75
Serum FGF23 (RU/L)
800
600
400
200
0
0
4
8
12
24
48
72
96
Time (months)
D
Codon 718 719 720 721 722
WT Ala
Amino acid Asn Gly Ile Ser
Mutant Ser
WT G
Nucleotide AAT GGT CA ATT AGT
Mutant T
E
720
Proband SPPQFRVNGSI SNFEEFQKA
H. Sapien SPPQFRVNGAI SNFEEFQKA
P. Trogloodytes SPPQFRVNGAI SNFEEFQKA
M. Muscul us SPPQFRVNGAI SNFEEFQKA
G. Gal l as SPPMFRVI GAMSNFEEFRKA
X. Tropi cal i s SPPQFRVI GAMSNFEEFHKA

1

2

Figure 2

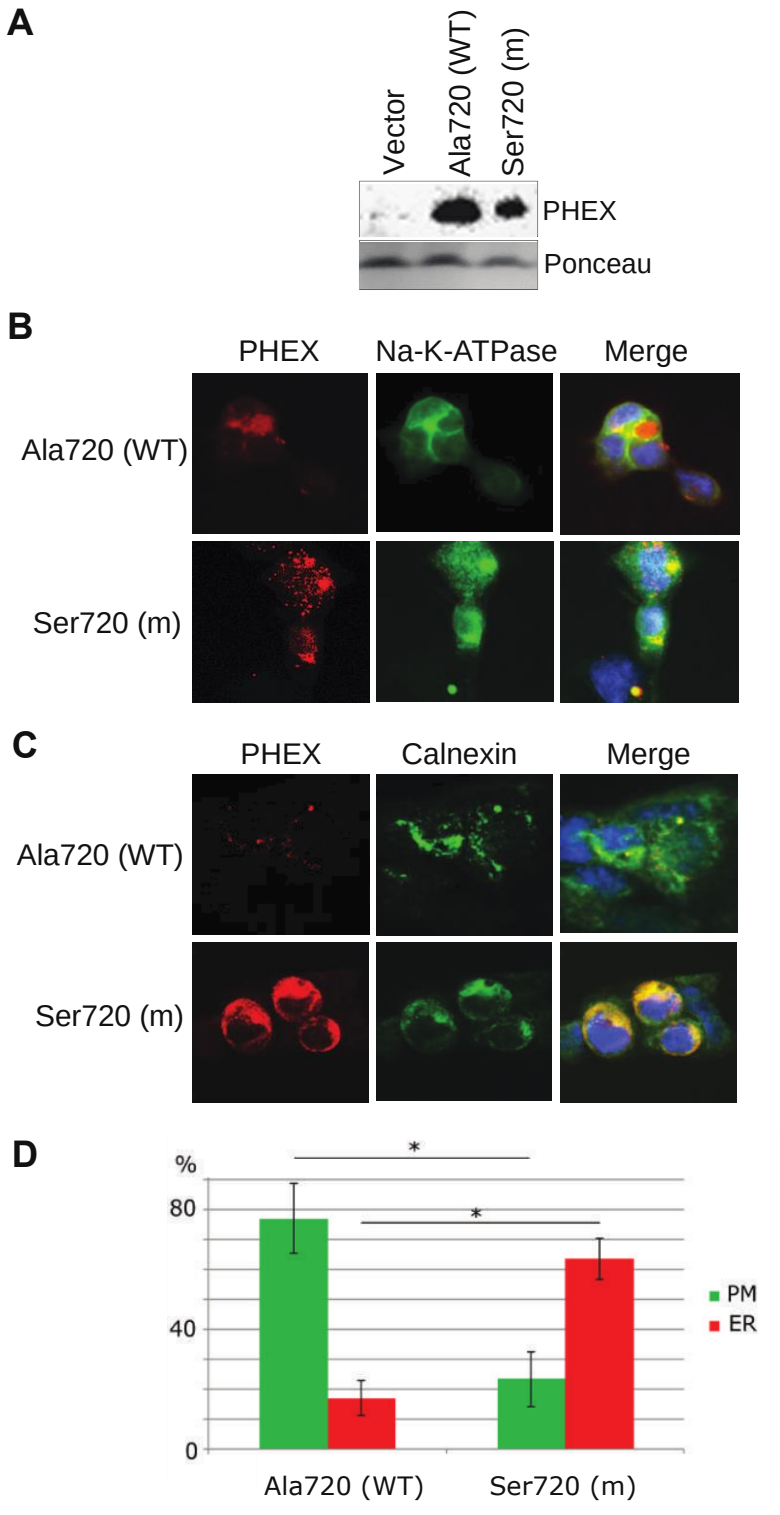
A
Vector
Ala720 (WT)
Ser720 (m)
PHEX
Ponceau
B
PHEX
Na-K-ATPase
Merge
Ala720 (WT)
Ser720 (m)
C
PHEX
Calnexin
Merge
Ala720 (WT)
Ser720 (m)
D
%
80
40
0
*
*
PM
ER
Ala720 (WT)
Ser720 (m)

1